Research Square

Preprints are preliminary reports that have not undergone peer review.
They should not be considered conclusive, used to inform clinical practice,
or referenced by the media as validated information.

Spectral Discrimination of Six Dominant Seaweed Species in the Intertidal Zone of GouQi Island

jianqu chen
Shanghai Ocean University
xunmeng li
Shanghai Ocean University
Kai Wang (kwang@shou.edu.cn)
Shanghai Ocean University
Shouyu Zhang
Shanghai Ocean University
Jian Zhang
Shanghai Ocean University
weicheng gao
Shanghai Ocean University

Research Article

Keywords: intertidal zone, dominant species, spectral analysis, support vector machine, distinction, fusion model

Posted Date: September 15th, 2021

DOI: https://doi.org/10.21203/rs.3.rs-877541/v1

License: This work is licensed under a Creative Commons Attribution 4.0 International License.
Read Full License

Abstract

Probing the coverage and biomass of seaweed is the basis for achieving sustainable utilization of nearshore seaweed resources. Unlike traditional sample surveys, remote sensing technology can realize dynamic monitoring on a large scale and for a long time. In this paper, we measured the spectral data of six dominant seaweed species in different dry and wet conditions in the intertidal zone of Gouqi Island: *Ulva pertusa*, *Sargassum thunbergii*, *Chondrus ocellatus*, *Chondria crassiaulis* Harv., *Grateloupia filicina* C. Ag., and *Hizikia fusifarme*. The different seaweed species were identified and analyzed by a combination of ANOVA and support vector machine (SVM). Fourteen common spectral parameters were used as input variables, and the input parameters were filtered by ANOVA. The samples were divided into a training set (266 samples) and a test set (116 samples) at a 3:1 ratio for input into the SVM model. The results showed that when the input parameters were NDVI (R_g,R_r), RVI (R_g,R_r), V_{re}, A_{be}, L_{be}, L_g, L_{re}, and R_r and the model parameters g=1.30 and c=2.85, the maximum discrimination rate of the six different wet and dry states of seaweed was 74.96%, and the highest accuracy was 93.94% when distinguishing different phyla of seaweed (g=6.85 and c=2.55). In addition, SVM is fused with XGBoost (eXtreme Gradient Boosting) by vote and further classified in combination with the selected parameters. The accuracy of the six seaweeds was 73.98% (vote mean score = 0.972). In this study, the spectral data of intertidal seaweed in different dry and wet states were classified for the first time to provide technical support for remote sensing monitoring of coastal zones and seaweed resource statistics.

Introduction

Seaweed, as a dominant species of nearshore ecosystems, plays an important role in the conservation of fishery resources and improvement of the water environment. Seaweeds are widely distributed along 25% of the world's intertidal rocky coastlines, providing a constant source of primary productivity for coastal ecosystems and serving as the foundation for nearshore habitat protection and ‘blue carbon’ sinks (Fiblee Dexter et al 2016). China's coastal intertidal zone is rich in seaweed resources, mainly *Ulva pertusa*, *Sargassum thunbergii*, *Chondrus ocellatus*, and *Hizikia fusifarme*. They mainly belong to Chlorophyta, Phaeophyta and Rhodophyta. In recent years, due to the dual influence of man-made factors such as near-shore sewage discharge, rough seaweed harvesting and natural factors such as global warming and ocean acidification, the amount of seaweed resources in China's coastal zone has been decreasing sharply year by year (Wang L. 2011).

To date, studies on the ecology of intertidal seaweed have mainly focused on the diversity composition and seasonal variation characteristics of seaweed communities in local areas, there are few studies on biomass statistics, and the research methods are mostly based on sample sampling, which has a heavy workload and small investigation area. In recent years, marine remote sensing technology has been widely used in coral monitoring and fishery resource assessment (Huang Y. et al 2019; Liu Y. et al 2016). According to Qin Song et al., one of the new trends in seaweed academics and applications is long-term ecological monitoring of seaweed through satellite and drone aerial photography (Li J. Song Q. et al 2020). Among them, spectral analysis, as one of the basic techniques of marine remote sensing, is a

prerequisite for remote sensing feature identification (Yuhui F et al 2008). Hyperspectral data provide continuous band reflectance, making it easy to distinguish between different feature characteristics (Wu J. et al 2011). The application of hyperspectral techniques to study seaweeds in coastal countries such as the United States, Japan and Australia started earlier. For example, Myers et al. conducted a comparative analysis of the spectral characteristics of nearshore corals and domain seaweed at Lee Stockton, Bahamas, in the Caribbean and explored the spectral variability between the dominant corals and seaweed, providing a method for remote sensing identification of corals (Myers M R et al 1999). To date, hyperspectral techniques have been widely used in the study of terrestrial plants but rarely used in the study of seaweed (Du Z. et al 2020; Liu C et al 2020; Sun H. et al 2019). Only Zheng (Zhang Z. 2014) measured the spectral data of seawater, *Ulva prolifera* and *Sargassum* in the Yellow and East China Sea, derived the spectral characteristics of the three and counted the area covered by *Ulva prolifera*. In addition, many spectroscopy studies have been conducted on seaweed, but they are not precise to specific seaweed "Species" (Cavanaugh K C et al 2010; Ishiguro E et al 2005; Bell T W et al 2015; THOMAS Ē.M. BELL 2015). On the other hand, since the study subjects are distributed in the intertidal zone, they will vary over time, showing different wet and dry states, which are different from exclusively terrestrial or aquatic plants. To provide theoretical guidance for the assessment of intertidal seaweed resources, this study was conducted by classifying seaweeds in different wet and dry states (at the dry-out time of two high tides). No studies have been reported on the spectra of seaweed in different dry and wet states.

The intertidal seaweed resources along the coast of Gouqi Island in Shengsi County, Zhejiang Province, China, are relatively abundant, and the dominant seaweed mainly includes *Sargassum thunbergii*, *Ulva pertusa*, *Chondrus ocellatus* and *Hizikia fusifarme* (Zeng Y. et al 2013). To investigate the characteristics of the intertidal seaweed community of Gouqi Island, this paper investigates the spectral characteristics of six dominant seaweed species (*Sargassum thunbergii*, *Ulva pertusa*, *Chondrus ocellatus*, *Chondria crassiaulis*, *Hizikia fusifarme*, and *Grateloupia filicina*) of different phyla and different wet and dry states. The spectral reflectance characteristics of different seaweeds were analyzed, and 14 common spectral parameters were screened by variance analysis combined with variable reduction (VACVR). The spectral parameters screened were used to classify seaweeds, and a discrimination model was established to identify different species of seaweeds, which can provide technical support for remote sensing monitoring of intertidal seaweeds. To fit the actual situation, the spectra of six seaweeds in different dry and wet states are considered. Mainly divided into three dries out degrees: measured immediately after collection (wettest), measured after waiting for the two highest tide times after collection (driest), measured at any time within the waiting time for two high tides (moderately dry and wet).

Materials And Methods

Sample Collection and Preparation

Located in the southern Ma’an Islands in Shengsi County, Zhejiang Province, China, Gouqi Island has many reefs and rich biological resources in nearby waters, with unique natural geomorphology and

intertidal biodiversity features. The nearshore substrate is mostly rocky reefs, where many seaweeds grow and thrive, forming a complex nearshore marine ecosystem (Zuli W et al 2019). The seaweeds of Gouqi Island are most abundant in summer and autumn every year, and the survey period of this study is October 17–24, 2019, and January 1–7, 2021, 11:30 – 13:30 (UTC/GMT + 08:00). To reduce the influence of human activities and mussel farming on the growth of intertidal seaweeds and to ensure that the survey sites are representative, Miaogan Village (122.793125E, 30.723037N) and Houtou Bay (122.777962E, 30.727135N) were selected as the seaweed spectral data collection sites (Fig. 1).

Spectral data collection of dominant intertidal seaweed species was performed by an ASD Field Spec Handheld (Field Spec Handheld, ASD, USA). Its wavelength observation range is 325 nm-1075 nm, including the visible and near infrared bands that are widely used for vegetation research, with a spectral sampling interval of 1 nm, a spectral resolution of 3 nm, and a field of view of 25°.

Spectrometer optimization was performed every 10–15 min, and dark currents were collected every 5 min. Before the spectral measurement of the feature, the spectrometer was calibrated against a reference whiteboard to obtain a horizontal straight line with a reflectivity of 1, and then the spectral measurement of the target feature was performed. After successful completion of spectrometer optimization, dark current acquisition, and whiteboard correction, the spectrometer can be pointed at the target feature, and the spectral data of the target feature can be collected and stored in real time. Three measurement points were randomly selected for the target feature during spectroscopy, and five sets of spectral data were read at 10 s intervals for each measurement point. A total of 400 target spectral data points were collected in this study. After completing the in situ spectral measurements, some of the experimental seaweeds were collected, brought back to the laboratory to determine their biological parameters and recorded (Chen C. 2019).

Statistical Analysis

Measured spectral data in the UV band before the wavelength of 400 nm are noisy, and after 900 nm is affected by water vapor absorption, they should be eliminated (Chen Q. et al 2015). The mean value of the feature spectral curve is used as the effective spectral value to reduce the effect of noise and randomness.

The spectral reflectance curves of seaweed (a total of six seaweed species) were represented by principal component analysis (PCA) using the first principal component, which was used to analyze the similarities and differences among seaweed spectra. The six seaweeds were grouped, and the pairwise difference (P) between 14 spectral parameters of different seaweeds was obtained by ANOVA (followed by Tukey’s post hoc test for multiple comparisons). The spectral parameters were screened by P and used for classification.

The machine learning method can directly apply the raw spectral data of the features for modeling and prediction and use the overall characteristics of the raw spectra as the discriminative basis for substrate feature classification. The support vector machine (SVM) is a supervised learning method for binary

classification of data, and its decision boundary is the maximum margin hyperplane solved for the test set, allowing for dimensionality reduction of high-dimensional data (Nguyen Quang H et al 2021), which has the advantages of small sample size, generality, and robustness (Liu B. et al 2020). Zhang et al. (Zhang J. et al 2020) used different classification methods, such as the spatially adaptive full variance method based on multiple logistic regression and the spatial feature extraction method based on superpixels, to classify spectral remote sensing images and concluded that the SVM algorithm using only spectral information can effectively differentiate spectral data. The method of selecting parameters can effectively reduce the amount of computation. In this paper, we apply the soft-margin algorithm to build a support vector machine model to distinguish seaweed spectral data quickly and accurately.

Result

The dominant seaweeds in the intertidal zone of Gouqi Island were selected for spectroscopic measurements, among which *Ulva pertusa* was a representative seaweed species of Chlorophyta (Fig. 2a); *Sargassum thunbergii* and *Hizikia fusifarme* were representative seaweed species of Phaeophyta (Fig. 2b, 2e); and *Chondrus ocellatus*, *Chondria crassiaulis* and *Grateloupia filicina* were representative seaweed species of Rhodophyta (Fig. 2c, 2d, 2f). Their original spectral features are analyzed separately, and based on this, more extensive data are applied for separability analysis and establishment of discriminatory criteria.

a) *Ulva pertusa*; b) *Sargassum thunbergii*; c) *Chondrus ocellatus*; d) *Chondria crassiaulis*; e) *Hizikia fusifarme*; f) *Grateloupia filicina.*

Spectral Characteristics of Six Species

The spectral curves of the above six species of seaweed were measured by an ASD spectrometer. After preprocessing the spectral data of seaweed in different dry and wet states, the spectral curves of six species of seaweed were drawn (Fig. 3).

a) *Chondria crassiaulis*; b) *Chondrus ocellatus*; c) *Ulva pertusa*; d) *Sargassum thunbergii*; e) *Grateloupia filicina*; f) *Hizikia fusifarme.*

Six species in the visible wavelength band with low reflectance; At the wavelength of 554 nm, *Ulva pertusa* shows a reflection peak; At wavelengths of 596 nm and 643 nm, *Sargassum thunbergii, Hizikia fusifarme* showed reflection peaks; at 648 nm and 678 nm, *Chondrus ocellatus*, showed reflection peaks, the reflectance of them is within 30%; In the near-infrared band, the reflectance of six species of seaweed increases suddenly, up to 80%, and the reflectance is higher in the infrared band. According to the literature, the pigments of different phylum species are different (Maxwell K and Johnson G N 2000; Liu Q. 2019) (Table 1).

Table 1
The similarities and differences of some pigments in different species.

Category	Contained pigment
Phaeophyta	Phlorotannins, Carotenoids, chlorophyll a
Chlorophyta	Carotenoids, chlorophyll a, chlorophyll b
Rhodophyta	Carotenoids, Phycoerythrin, chlorophyll a

In this paper, the spectral waveforms of each seaweed are similar to the corresponding phylum reported in many studies. Generally, the distribution of seaweed offshore is as follows: the distribution of green seaweed is the shallowest, followed by brown seaweed, and red seaweed is often in the deepest water layer (Cheng X. 2019). seaweed growing in shallow coastal zones evolved specific mechanisms to resist strong light damage (Melis A 1999). In Phaeophyta, Phlorotannins can resist solar radiation as a kind of light shielding material (Wang Y. et al 2020). In addition, fucoxanthin in Phaeophyta can absorb short wavelength light (Wu Y. et al 2020), so the shading effect of phlorotannins and fucoxanthin may be the main reason for the low reflectivity of Phaeophyta compared with Rhodophyta and Chlorophyta in the wavelength range of 400–900 nm. The spectral curves of the *Sargassum thunbergii* and *Hizikia fusifarme* are very similar to that of reported seaweed. There are fine bimodal patterns at 600 nm and 650 nm, and the maximum reflectivity in the near infrared and infrared bands is 40% (Zhang Z. 2014; Ishiguro E et al 2005; Stéphane Maritorena et al 1994; Cavanaugh K C et al 2010) (Fig. 3).

In the range of 400–700 nm, the spectral reflectance curve of *Ulva pertusa* has a peak. The reflectance of the blue-violet band (400–492 nm) is the lowest, which is 3.6–7.72%. In the yellow green band (492–597 nm), due to the reflection of chlorophyll in seaweed, the spectral curve has a broad and prominently high value, approximately 25.27%. In the orange-red band (597–700 nm), the reflection first decreases and then increases, with a minimum value of 5.78 at 669 nm. In the red edge band (670–760 nm), the reflectivity increases sharply to 83.4% (Fig. 3).

Chlorophyll in seaweed can absorb most of the visible light, but when the wavelength is greater than 700 nm, the reflection mechanism of each cell is similar to a small corner reflector, so the cell's structure is also an important factor affecting the reflectivity (Horler D N H et al 1983). Therefore, the electromagnetic reflectance of *Ulva pertusa* in the red-edge band can rapidly increase from 5–80%. Due to the lack of active fluorescence absorption on the surface of seaweed (Filella I and Penuelas J 1994), the reflectance of the near infrared shortwave band (780–900 nm) is approximately 80%.

In the range of 400–700 nm, *Sargassum thunbergii* and *Hizikia fusifarme* have three maximum reflectance values. In the blue-violet band (400–492 nm), the reflectivity is low, approximately 0.85–1.4%. In the yellow-green band (492–597 nm), the reflectivity increases continuously and reaches a maximum at 596 nm, which is approximately 3.74%. In the orange-red band (597–700 nm), there is another maximum at 643 nm, and the reflectivity is approximately 2.19%. In the red-edge band (670–760 nm),

due to the influence of cell structure, the reflectivity increases sharply, and the highest is approximately 34.91%. The reflectivity in the short wave band (780–900 nm) is approximately 35%.

In the range of 400–700 nm, the total reflectance of *Chondrus ocellatus*, *Chondria crassiaulis* and *Grateloupia filicina* is high in the visible light range, and there are two maxima. In the blue-violet band (400–492 nm), the reflectivity is approximately 30.4-33.79%. In the yellow-green band (492–597 nm), the reflectance first decreases and then increases, and there is a minimum at 536 nm, which is approximately 12.55%. In the orange-red band (597–780 nm), there are two maxima at 648 nm and 678 nm, and the reflectivity is approximately 33.87% and 32.31%, respectively. In the red edge band (670–760 nm), due to the influence of cell structure, the reflectivity rises sharply, and the highest is approximately 86.04%. In the near-infrared (780–900 nm) shortwave band, the reflectivity is maintained at approximately 85%.

Analysis and Optimal Screening of Spectral Parameters of Seaweeds

The spectral parameters of the 14 commonly used compounds were screened by ANOVA. The original data were analyzed by variance, and the significance between different seaweed species (P, Supplementary material) was obtained. The smaller the P, the greater the significance. The 14 parameters (Table 2) were used as input variables to derive the initial discriminant accuracy. The corresponding parameters are eliminated according to P from large to small until the model reaches the optimal discriminative accuracy.

Table 2
14 commonly used spectral parameters.

Parameters types	Parameters	Symbol	Definition
Location parameters	Green peak amplitude	R_g	Maximum reflectivity of 510–560 nm in green light range
	Green peak loction	L_g	Wavelength of green peak in the green range of 510–560 nm
	Red valley amplitude	R_r	Maximum reflectivity of 640–680 nm in red light range
	Red valley location	L_r	Wavelength corresponding to Red Valley 640–680 nm in red light range
	Red edge amplitude	V_{re}	Maximum value of first order differential in red edge 680–760 nm
	Red edge location	L_{re}	Wavelength corresponding to red edge amplitude
	Blue edge amplitude	V_{be}	First order differential maximum in 490–530 nm of blue edge
	Blue edge location	L_{be}	Band length corresponding to blue edge amplitude
Area parameters	Red edge area	A_{re}	Sum of first order differential values in the range of red edge
	Blue edge area	A_{be}	Sum of first order differential values in the range of blue edge
Vegetation index Parameters	R_g/R_r	RVI (R_g, R_r)	Amplitude ratio of green peak to Red Valley
	A_{re}/A_{be}	RVI (A_{re}, A_{be})	Area ratio of red edge to blue edge
	$(R_g\text{-}R_r)/(R_g+R_r)$	NDVI (R_g, R_r)	Normalized ratio of green peak to Red Valley amplitude
	$(A_{re}\text{-}A_{be})$ $/(A_{re}+A_{be})$	NDVI (A_{re}, A_{be})	Normalized ratio of red edge area to blue edge area

To study the changes in 14 spectral parameters of different seaweed, the first principal component of each spectral parameter in different seaweed species was calculated, and the corresponding characteristics of each spectral parameter of different seaweeds were analyzed by using this value. Each seaweed was subjected to principal component analysis, and their loadings were all greater than 90%,

indicating that the first principal component can effectively express the information in each seaweed dataset.

The positions of the green peak, red valley, blue edge and red edge are marked on the spectral curve, as shown in Fig. 4. To observe the trends of the spectral parameters more clearly, the four regions corresponding to the reflection spectra and the first-order derivative spectra in regions (a), (b) and (c) and (d) in Fig. 5 are enlarged to obtain four spectral enlargements.

a) Enlarged image of the first-order differential spectrum at 490–530 nm (blue border area); b): Enlarged image of the spectrum at 510–560 nm (green peak area); c): Enlarged image of the spectrum at 640–680 nm (red valley area); d): Enlarged image of the first-order differential spectrum at 680–760 nm (red area).

Figure 4 shows that there were obvious differences in seaweed spectra among different phyla, while there were small differences among the same species. For example, in (b), the green peak amplitude R_g: in Rhodophyta, *Chondria crassiaulis*, *Chondrus ocellatus* and *Grateloupia filicina*. were − 0.8063, − 0.8247 and − 0.8158, respectively; in Phaeophyta, the values of *Sargassum thunbergii* and *Hizikia fusifarme* were − 0.7590 and − 0.7555, respectively; and *Ulva pertusa* was − 0.5706. The location of green peak location L_g: in the Rhodophyta, the values of *Chondria crassiaulis*, *Chondrus ocellatus* and *Grateloupia filicina*. were 535.6500 nm, 521.7119 nm and 526.5200 nm, respectively; among Phaeophyta, *Sargassum thunbergii* and *Hizikia fusifarme* were 559.8025 and 560.0000, respectively; and *Ulva pertusa* was 551.1475. The difference in spectral curves among the same phylum was smaller than that among different phyla.

The ANOVA results (Supplementary material) were averaged to represent the P of the corresponding parameters (Table 3). The 14 parameters were selected according to significance, and the parameters with small significance difference were eliminated one by one until the model reached the optimal discriminant accuracy; The order of significance of 14 parameters was as follows: NDVI(R_g, R_r)、RVI、R_g, R_r)、V_{re}、L_{be}、A_{be}、L_g、L_r、R_r、L_{re}、R_g、NDVI(A_{re}, A_{be})、A_{re}、V_{be}、RVI(A_{re}, A_{be}) (Table 3).

Table 3
P of different spectral parameters.

Spectral parameters	Average P
NDVI (R_g, R_r)	0.0300
RVI (R_g, R_r)	0.0340
V_{re}	0.0425
L_{be}	0.0672
A_{be}	0.0739
L_g	0.0831
L_r	0.0986
R_r	0.0986
L_{re}	0.1261
R_g	0.1323
NDVI (A_{re}, A_{be})	0.1581
A_{re}	0.1687
V_{be}	0.2222
RVI (A_{re}, A_{be})	0.4391

Support Vector Machine (SVM)

Because the growth environment of intertidal seaweed is different from that of terrestrial and aquatic plants, the rise and fall of tides will affect the spectral reflection curve of seaweed. To eliminate the influence of seawater on the discrimination results and expand the application scenarios, it is necessary to carry out spectral determination of seaweed with different drying degrees. Among them, class 1 represents *Chondrus ocellatus*, class 2 represents *Chondria crassiaulis*, class 3 represents *Grateloupia filicina*, class 4 represents *Sargassum thunbergii*, class 5 represents *Hizikia fusifarme*, and class 6 represents *Ulva pertusa*. A total of 382 groups of data were randomly divided into a training set and a testing set at a ratio of 3:1.

In this paper, the construction of the SVM-based classification model is based on Pytharm in the environment of Python 3.7, mainly using the joblib module of sciket learn SVM (sklearn SVM). The type of kernel function is RBF, and its value equals 2; degree = 3; coef0 = 0.

Table 4
Selection results of spectral characteristic parameters.

Rejected parameters	Parameter quantity	Accuracy (%)
——	14	40.89
NDVI (A_{re}, A_{be}), A_{re}, V_{be}, RVI (A_{re}, A_{be})	10	68.34
R_g, NDVI (A_{re}, A_{be}), A_{re}, V_{be}, RVI (A_{re}, A_{be})	9	66.02
L_{re}, R_g, NDVI (A_{re}, A_{be}), A_{re}, V_{be}, RVI (A_{re}, A_{be})	8	74.96
R_r, L_{re}, R_g, NDVI (A_{re}, A_{be}), A_{re}, V_{be}, RVI (A_{re}, A_{be})	7	71.96
L_r, R_r, L_{re}, R_g, NDVI (A_{re}, A_{be}), A_{re}, V_{be}, RVI (A_{re}, A_{be})	6	64.57

From Table 4, when all 14 parameters were used to distinguish seaweed species, the effect was the worst, only 40.89%. When the parameters with smaller significance (larger P) were eliminated one by one, the discrimination accuracy increased. Until the four parameters were eliminated, the highest discrimination accuracy was 74.96%. Then, with the decrease in input parameters, the accuracy of discrimination decreased.

When NDVI(R_g, R_r), RVI(R_g, R_r), V_{re}, L_{be}, A_{be}, L_g, L_r, and R_r are selected as input parameters, the optimal parameters of the model are g = 1.30 and c = 2.55, and the accuracy is 74.96% (Fig. 6). By outputting the misclassified seaweed species, it was found that there was more misclassification between Rhodophyta and Phaeophyta, especially between different dry and wet conditions; there was no error in seaweed classification among different phyla.

When the same input parameters were selected and the model parameters of different phyla (Chlorophyta: *Ulva pertusa*; Phaeophyta: *Sargassum thunbergii, Hizikia fusifarme*; Rhodophyta: *Chondrus ocellatus, Chondria crassiaulis*, *Grateloupia filicina*) were optimized, the results showed that when g = 6.85 and C = 2.55, the discrimination accuracy was the highest, which was 93.94% (Fig. 7).

Fusion model

Because the classification results of only a single model are unsatisfactory, we use the model fusion method to further verify the six kinds of seaweed. SVM and XGBoost are fused by the vote algorithm to obtain the fusion model. By bringing the parameters filtered by SVM into the fusion model, all samples are divided into a training set and test set at a ratio of 7:3, and the classification results and accuracy are calculated. The vote score mean is 97.211%, and the classification results are shown in Fig. 7.

From the classification results, the classification of Category 3 (*Ulva pertusa*) is correct. There were 12 mismatches among category 1 (*Chondria crassiaulis* Harv.), category 2 (*Chondrus ocellatus*) and category 5 (*Grateloupia filicina* C. Ag.). There were 20 mismatches in Category 4 (*Sargassum thunbergii*)

and category 6 (*Hizikia fusifarme*). The overall accuracy was 73.98%(Fig. 8), which further confirms the difficulty of spectral data in processing the classification of the same seaweed species.

Discussion

With increasing *Ulva pertusa* thickness, the reflectance of *Ulva pertusa* and *Ulva prolifera* is similar, and the reflectance of the yellow-green band and near-infrared band increases with increasing seaweed thickness (Zhenglong Z 2014; Yanfang Xiao et al 2019). In this paper, the spectral data of *Ulva pertusa* with different layers were measured. The results showed that with the increase in the number of layers, the spectral curve of *Ulva pertusa* was approximately 550 nm in the near-infrared band, and the reflectance increased exponentially. When it was superposed to three layers, the spectral reflectance of the yellow green band was the highest, approximately 25%, and the near-infrared band was approximately 80%. The spectral reflectance curve of *Ulva pertusa* increased to 4, 5 and 6 layers and was similar to that of 3 layers, indicating that the spectral reflectance curve of *Ulva pertusa* reached a saturation state when the number of layers reached 3, which was very similar to that of *Ulva prolifera* with different thicknesses. Liu Qing (2019) studied the physiological and biochemical responses of intertidal seaweed to copper stress, and the results showed that the chlorophyll content decreased with increasing Cu2 + in *Ulva pertusa* (Qin L 2019). Therefore, the chlorophyll content in *Ulva pertusa* (yellow-green band) can be used as an indicator of heavy metal pollution in coastal zones.

Although there are few studies on the spectral characteristics of Rhodophyta, it can be found from other studies (such as corals) that Rhodophyta on the surface of bleached coral (Qidong C et al 2015; Filella I and Penuelas J 1994). Through comparative analysis, it is not difficult to find that the spectral characteristics of Rhodophyta are very similar. The minimum value of Rhodophyta in the green band may be due to the absorption of green light by phycoerythrin (Yonghu W 2020).

In summary, the contents of chlorophyll and carotenoids in the same phylum were similar, and the differences among different phyla were obvious. Therefore, it is considered that the same spectrum phenomenon of foreign matter may occur among the same phylum. The higher the plant activity is, the better the chlorophyll activity is, and the higher the spectral reflectance is in the corresponding band (Yanlin T et al 2003), so it is necessary to measure the spectrum of the same seaweed in different seasons to further explore the seasonal variation of the spectral reflectance curve of seaweed. In addition, it has been confirmed that there are gender differences in light adaptation in seaweed (Kuster A. et al 2005). However, the effect of seaweed sex on the spectrum is not considered in this paper, and a follow-up study needs to be supplemented.

Conclusion

In this paper, the spectral data of *Hizikia fusifarme*, *Ulva pertusa*, *Chondria crassiaulis*, *Sargassum thunbergii* and *Grateloupia filicina* on Gouqi Island were analyzed, and the differences in the spectral characteristics of six seaweed samples were obtained. The main reason was the difference in pigment

content in seaweed, and the spectral reflectance curves of the same phylum of seaweed were very similar. In addition, the ANOVA results showed that the differences between seaweeds of the same phylum were not significant ($p > 0.05$), while the differences between seaweeds of different phyla were significant ($p \leq 0.05$).

The support vector machine (SVM) classification model can be used in collaboration with manual identification to identify different seaweed species and improve identification efficiency and accuracy. NDVI(R_g,R_r)、RVI、R_g,R_r、V_{re}、L_{be}、A_{be}、L_g、L_r、R_r were selected as input parameters, and the SVM model constructed with Gaussian kernel function could better distinguish the six seaweed species with an accuracy of 74. 96% when the model parameters c = 1.30 and g = 2.85. In misclassification, through the fusion model, the classification accuracy is 73.98%. The difference in seaweed spectrum among the same phylum was small, and the misclassification was large. However, the difference in seaweed spectrum among different phyla was large, and the error rate of misclassification result was low. Using the same method to distinguish the phyla of seaweed (Chlorophyta, Phaeophyta, Rhodophyta), the accuracy reached 93.94%.

In this paper, spectral analysis and classification of dominant seaweed species with different degrees of dryness and wetness on Gouqi Island are carried out, which has good practicability to provide technical support and a partial data basis for remote sensing of intertidal seaweed. The pigment and spectral response mechanisms of different species of the same phylum need to be further studied.

Declarations

AUTHOR CONTRIBUTIONS

KW and SZ conceived and designed the experiments. JC and XL provided the tissue samples. JC performed the experiments and analyzed the data with the help of KW and SZ. JC wrote the manuscript with the advice of XL, JZ, and WG. All authors provided editorial advice and agreed that this version of the manuscript was acceptable for submission.

FUNDING

The authors received financial support from the China Agriculture Research System (CARS-50).

ACKNOWLEDGMENTS

We appreciate the support of our funding agency, the China Agriculture Research System (CARS-50). We also thank the editor and the anonymous reviewers, whose comments significantly improved the manuscript.

References

Bell T W, Cavanaugh K C, Siegel D A (2015). Remote monitoring of giant kelp biomass and physiological condition: An evaluation of the potential for the Hyperspectral Infrared Imager (HyspIRI) mission. *Remote Sens Environ* 218-228. doi: 10.1016/j.rse.2015.05.003

Cavanaugh K C, Siegel D A, Kinlan B P, et al (2010). Scaling giant kelp field measurements to regional scales using satellite observations. *Marine Ecology Progress* 403:13-27. doi: 10.3354/meps08467

Cavanaugh K C, Siegel D A, Kinlan B P, Reed DC (2010). Scaling giant kelp field measurements to regional scales using satellite observations. *Mar Ecol-Prog Ser* 403(mar.22):13-27. doi: 10.3354/meps08467

Chen C. (2019). Estimation of wheat biomass and yield based on UAV images. Yangzhou University.

Chen Q., Deng R., Qin Y., Xiong L., He Y. (2015). Analysis of spectral characteristics of coral under different growth patterns. *Acta Ecologica Sinica* 35(10):3394-3402. doi: 10.5846/stxb201306261783

Cheng X. (2019). Response of photosynthetic activity of large seaweed to different environmental conditions. Shanghai Ocean University.

Du Z., Wang L., Bao Y., Zhou X. (2020). Analysis of Hyperspectral Characteristics of *Phragmites australis* and *Spartina alterniflora* Leaves in Typical Beach. *Chinese Journal of Agrometeorology* 41(06):393-402. doi: 10.3969/j.issn.1000-6362.2020.06.006

Fiblee-Dexter, K, Feehan CJ, et al, (2016). Large-scale degradation of a kelp ecosystem in an ocean warming hotspot[J]. *Mar Ecol-Prog Ser*, 543:141-152. doi: 10.3354/meps11554

Filella I, Penuelas J (1994). The red edge position and shape are indicators of plant chlorophyll content, biomass and hydric status. *Int J Remote Sens* 15(7):1459-1470. doi: 10.1080/01431169408954177

Horler D N H, Dockray M, Barber J (1983). The red edge of plant leaf reflectance. *Int J Remote Sens* 4(2):273-288. doi: 10.1080/01431168308948546

Huang Y., Yu K., Wang Y., Liu J., Zhang H. (2019). Progress of the study on coral reef remote sensing. *Journal of Remote Sensing* 2019, 23(06): 1091-1112. doi: 10.11834/jrs.20198110

Ishiguro E, Yoshimoto S I, Ishikawa D (2005). Monitoring of the Environment around Kagoshima Bay Using Remote Sensing Data -Development of Identifying Method for Seaweeds Growing Region. *J Agric Meteorol* 60(5):409-414. doi: 10.2480/agrmet.409

Kuster A., Schaible R., Schubert (2005). H.S. Sex-specific light acclimation of Chara canescens (Charophyta). *Aquat Bot* 83,(2):129-140. doi: 10.1016/j.aquabot.2005.05.009

Li J., Song Q., Liu F., Ding L., Liu Z. (2020). New trends in the research and applications of seaweed in response to global change. *Chinese Science Bulletion* 65(05):334-338. doi: 10.1360/TB-2019-0151

Liu B., Zuo X., Tan X., Yu A., Guo W. (2020). A deep few-shot learning algorithm for hyperspectral image classification. *Acta Geodaetica et Cartographica Sinica* 49(10):1331-1342. doi: 10.11947/j.AGCS.2020.20190486.

Liu C., Lin L., Yu C., Wu J. (2020). Research on Peanut Hyperspectral Image Classification Method Based on Deep Learning. *Computer Simulation* 37(03):189-192+283.

Liu Q. (2019). Physiological and biochemical responses of three intertidal macroalgae to heavy copper stress. Yantai University

Liu Yafei (2016). Marine remote sensing technology and its application research on fisheries. Zhejiang Ocean University

Maxwell K, Johnson G N (2000). Chlorophyll fluorescence a practical guide. *J Exp Bot* 51(345):659-668. doi: 10.1093/jexbot/51.345.659

Melis A (1999). Photosystem-□ damage and repair cycle in chloroplasts: what modulates the rate of photodamage?. *Trends Plant Sci* 4(4):130-135. doi: 10.1016/S1360-1385(99)01387-4

Myers M R, Hardy J T, Mazel C H, et al (1999). Optical spectra and pigmentation of Caribbean reef corals and macroalgae. *Coral Reefs* 18(2):179-186. doi: 10.1007/s003380050177

Nguyen Quang H. et al. (2021). Stacking segment-based CNN with SVM for recognition of atrial fibrillation from single-lead ECG recordings. *Biomed Signal Proces*, 68. doi: 10.1016/j.bspc.2021.102672

Stéphane Maritorena, André Morel, Gentili B (1994). Diffuse reflectance of oceanic shallow waters: Influence of water depth and bottom albedo. *Limnol Oceanogr* 39 (7):1689-1703. doi: 10.4319/lo.1994.39.7.1689

Sun H., Liu N., Xing Z., Zhang Z., Li M., Wu J. (2019). Parameter optimization of potato spectral response characteristics and growth stage identification. *Spectroscopy and Spectral Analysis* 39(06):1870-1877. doi: CNKI:SUN:GUAN.0.2019-06-040

Tang Y., Wu J., Huang J., Wang R., He Q. (2003). Variation law of hypersprctral data and chlorophyll II and carotenoids for rice in the mature process. *Chinese Society of Agricultural Engineering* (06):167-173. doi: CNKI:SUN:NYGU.0.2003-06-039

THOMAS Ē.M. BELL (2015). Quantifying intertidal macroalgae abundance using aerial photography on the Isle of Wight. Imperial College London.

Wang Lei (2011). Relationship between ecosystem of kelp beds and seasonal variation of fish assemblages in waters around Gouqi Island. ShangHai Ocean University.

Wang Y., Li J., Chuan Z., Zhong Z., Pang Y., Liu Z. (2020). Photosynthetic characteristics of floating seaweeds and their research progress. *Transactions of Oceanology and Limnology* (05):105-112. doi: 10.13984/j.cnki.cn37-1141.2020.05.014

Wu J., Peng D (2011). Advances in research on hyperspectral remote sensing forestry information extraction technology. *Spectroscopy and Spectral Analysis* 31(09):2305-2312. doi:10.3964/j.issn.1000-0593(2011)09-2305-08

Wu Y., Su J. (2020). Study on plant pigments by photoacoustic spectroscopy. *Spectroscopy and Spectral Analysis* (03):378-380. doi: 10.3321/j.issn:1000-0593.2002.03.008

Wu Z., Zhang S. (2019). Effect of Typhoon on the Distribution of Macroalgae in the Seaweed Beds of Gouqi Island, Zhejiang Province. *Journal of Agricultural Science and Technology* 21(09):159-168. doi: 10.13304/j.nykjdb.2018.0695

Yan F., Xiao, Jie Z., Ting W., Cui, et al (2019). Remote sensing estimation of the biomass of floating *Ulva prolifera* and analysis of the main factors driving the interannual variability of the biomass in the Yellow Sea. *Mar Pollut Bull* 140. doi: 10.1016/j.marpolbul.2019.01.037

Yuhui F, Qijun L, Baoru Z (2008). Spectroscopic analysis of oil spills at sea and satellite information distilling. *Journal of Remote Sensing* (06):1010-1016. doi: 10.3321/j.issn:1007-4619.2008.06.026

Zeng Y., Ma J., Chen B., Cai Y., Gao S. (2013). Survey on the community of benthic macroalgae on Gouqi Island of Zhejiang Province. *Acta Agriculturae ZheJiangensis* 25(05):1096-1102. doi: 10.3969/j.issn.1004-1524.2013.05.33

Zhang J., Chen Y. (2020). Overview of hyperspectral image classification methods. Journal of Nanjing University Natural Science 12(01):89-100. doi: 10.13878/j.cnki.jnuist.2020.01.011

Zhang Z. (2014). Remote sensing identification of *Ulva prolifra* and *Sargassum* and Evolution of green tide in the Yellow Sea and the East China Sea. East China Normal University.

Figures

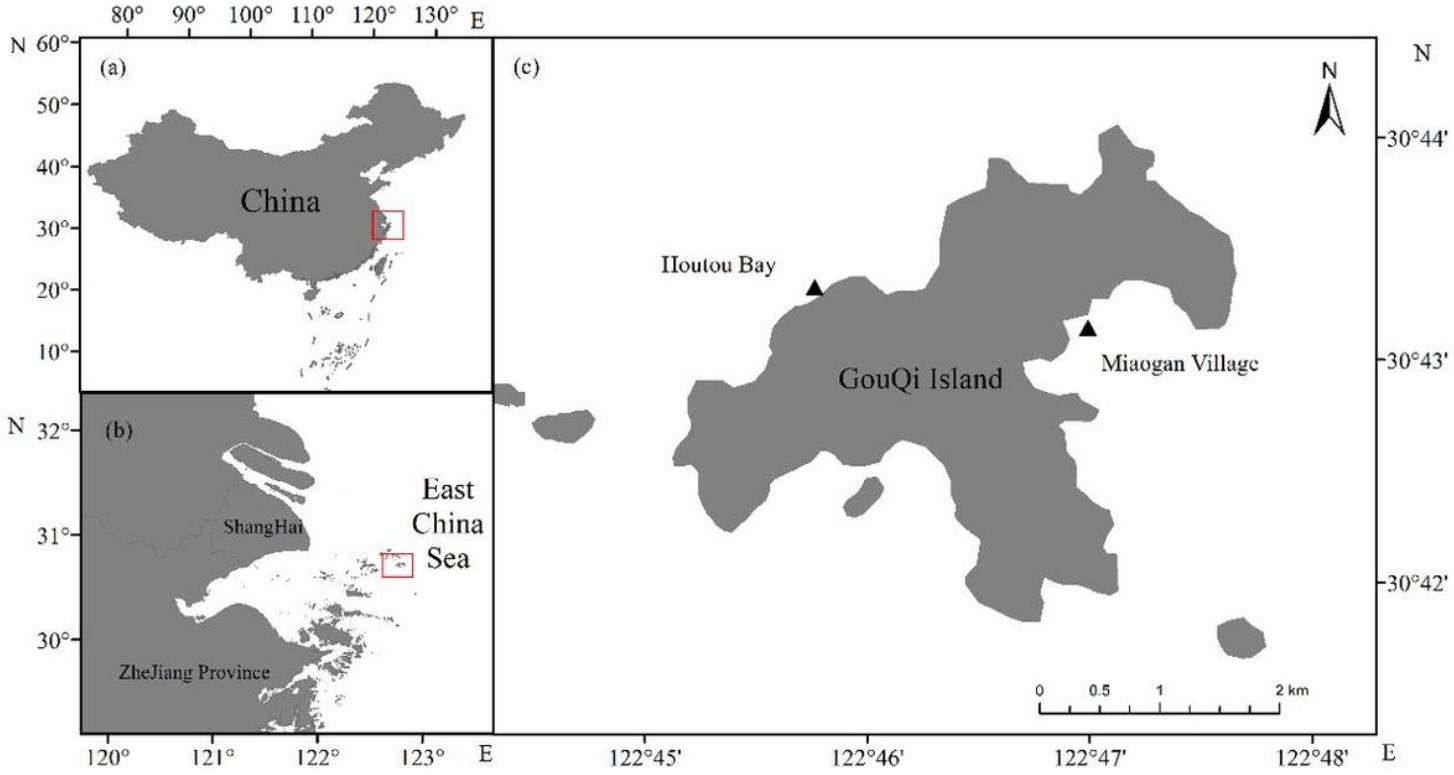

Figure 1

Location map of research. a) China; b) Yangtze River Estuary; c) Survey sites. Triangles indicate samplings.

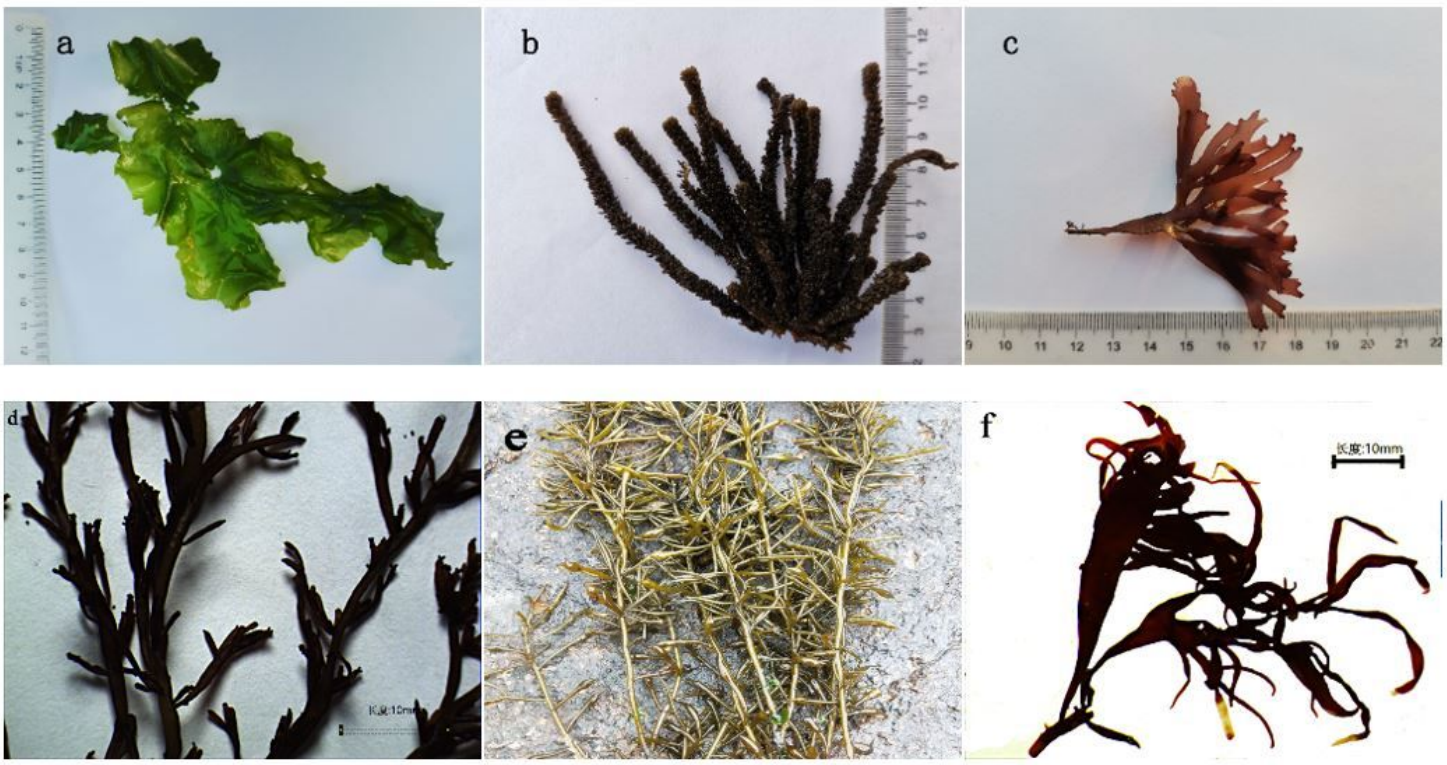

Figure 2

Dominant species in the intertidal zone of Gouqi Island. a) Ulva pertusa; b) Sargassum thunbergii; c) Chondrus ocellatus; d) Chondria crassiaulis; e) Hizikia fusifarme; f) Grateloupia filicina.

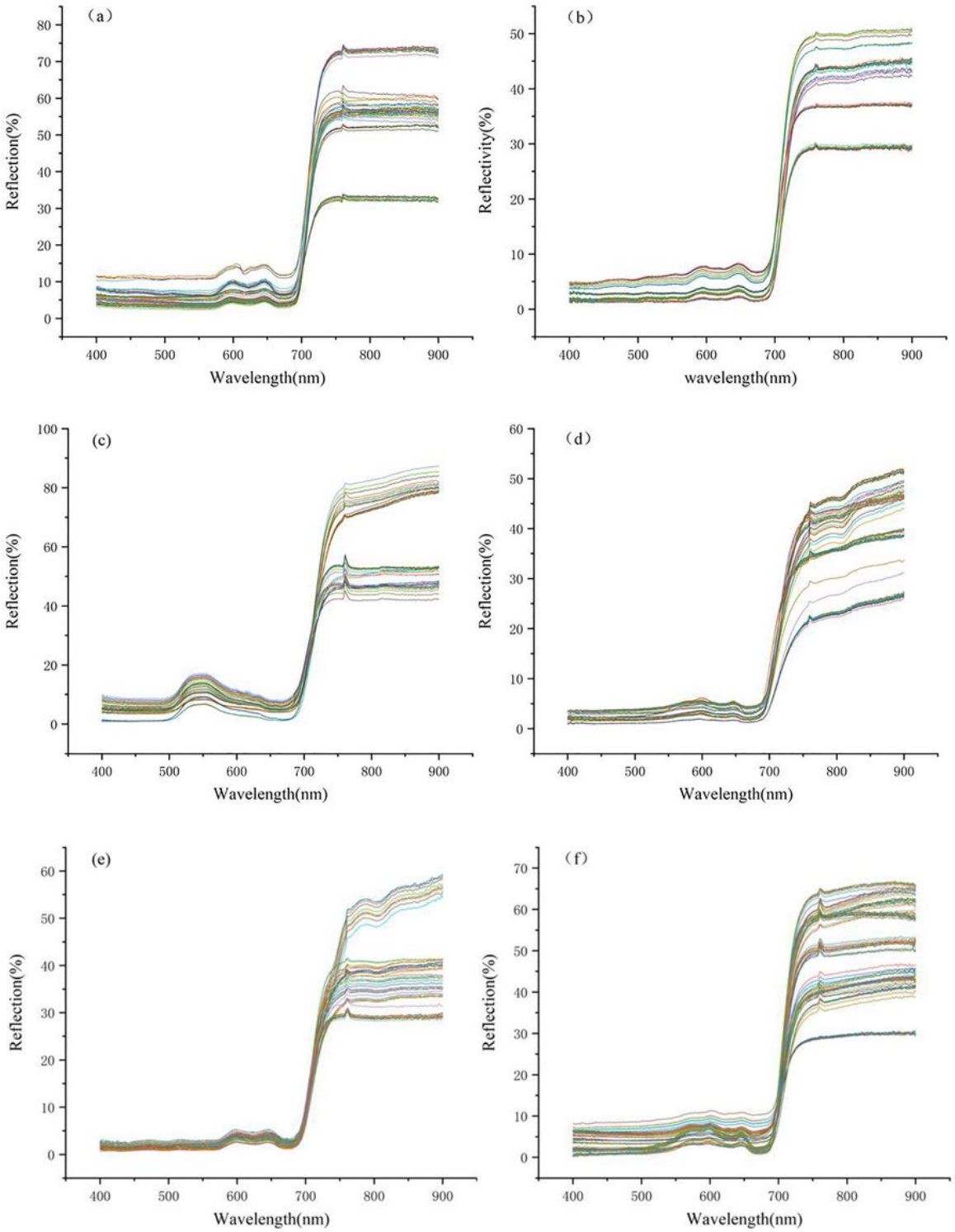

Figure 3

Spectral curves of six species of seaweeds. a) Chondria crassiaulis; b) Chondrus ocellatus; c) Ulva pertusa; d) Sargassum thunbergii; e) Grateloupia filicina; f) Hizikia fusifarme.

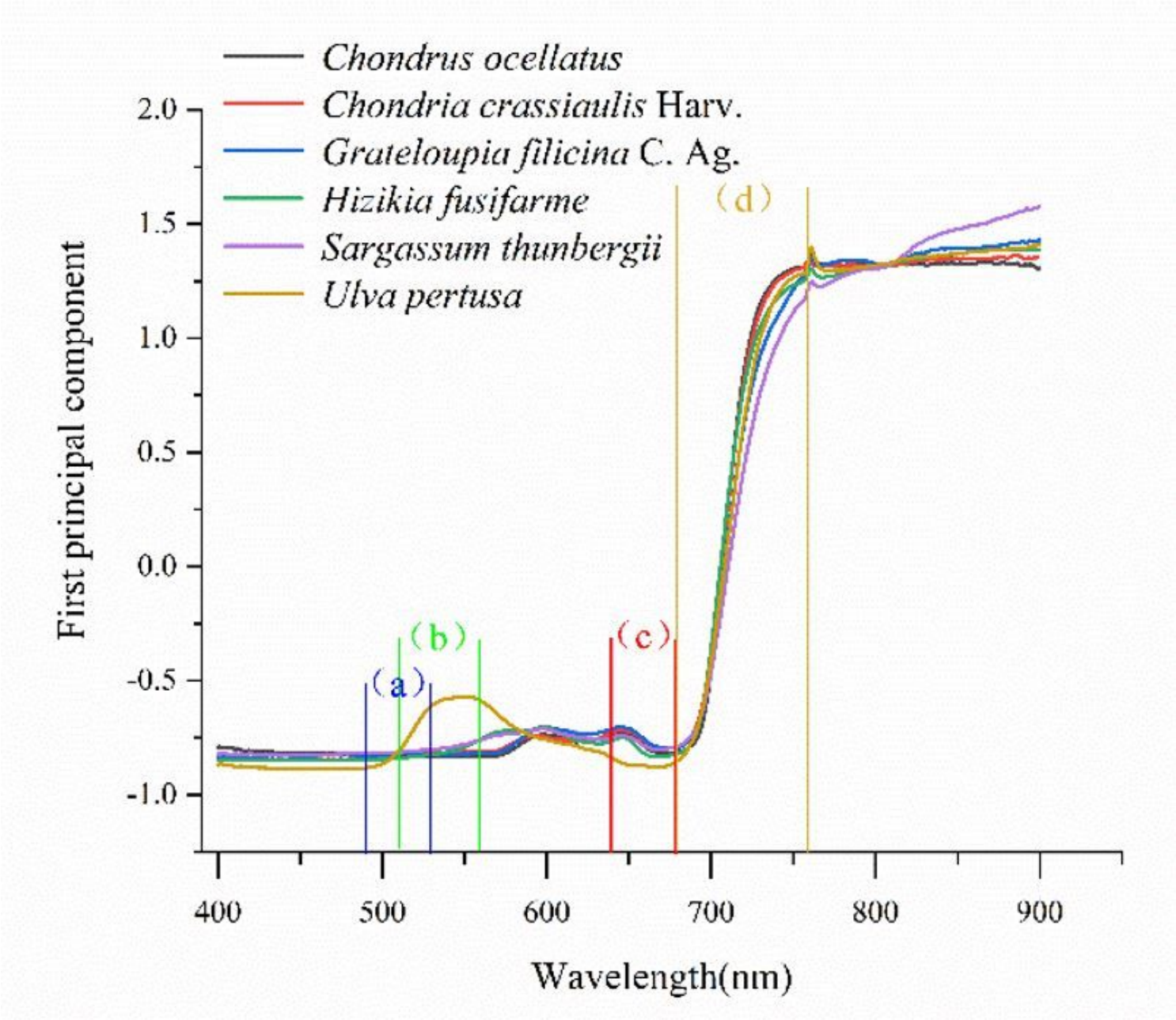

Figure 4

Spectral curves of the first principal component.

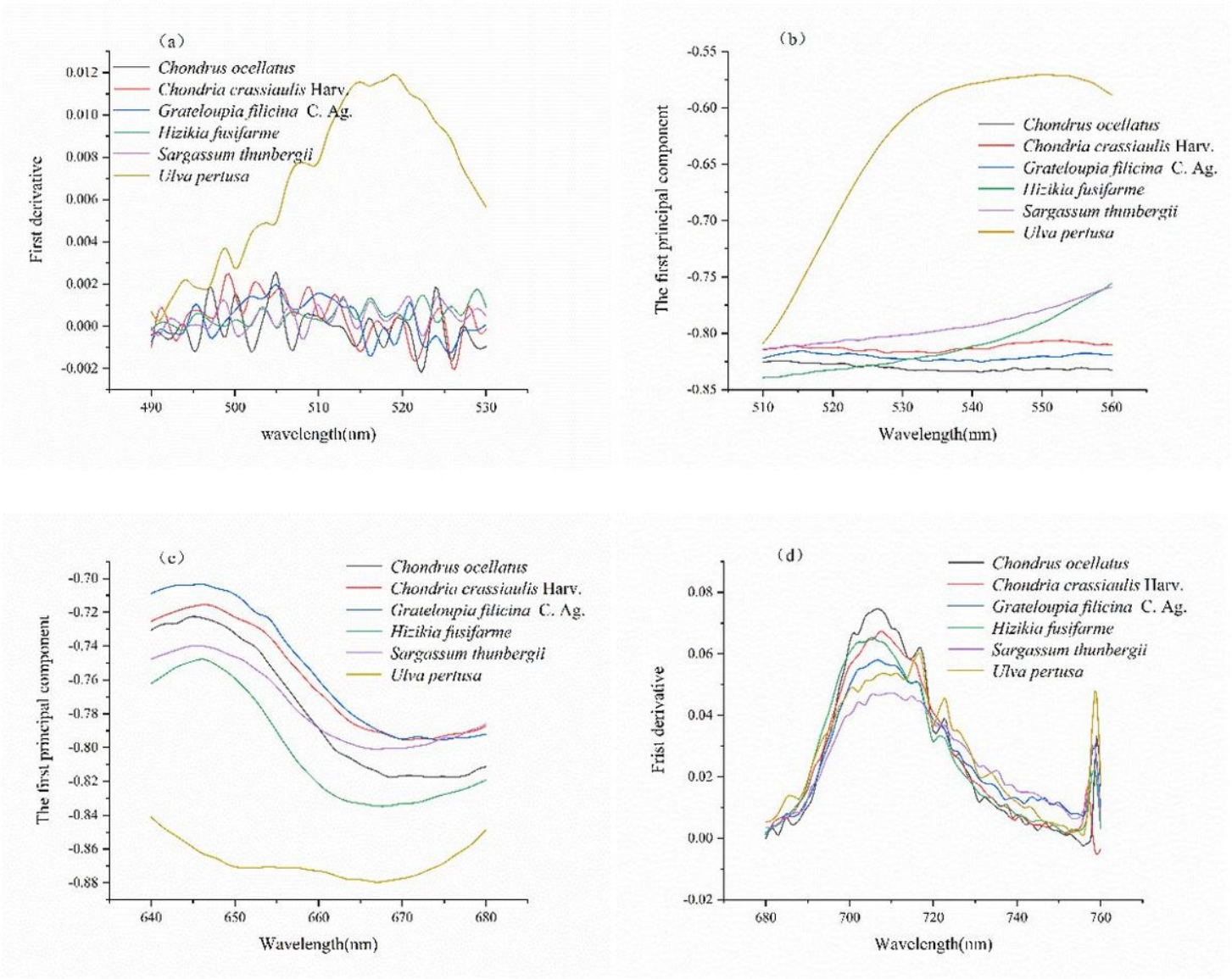

Figure 5

Spectrum enlarged view of green valley, red valley, blue edge and red edge locations. a) Enlarged image of the first-order differential spectrum at 490-530 nm (blue border area); b): Enlarged image of the spectrum at 510-560 nm (green peak area); c): Enlarged image of the spectrum at 640-680 nm (red valley area); d): Enlarged image of the first-order differential spectrum at 680-760 nm (red area).

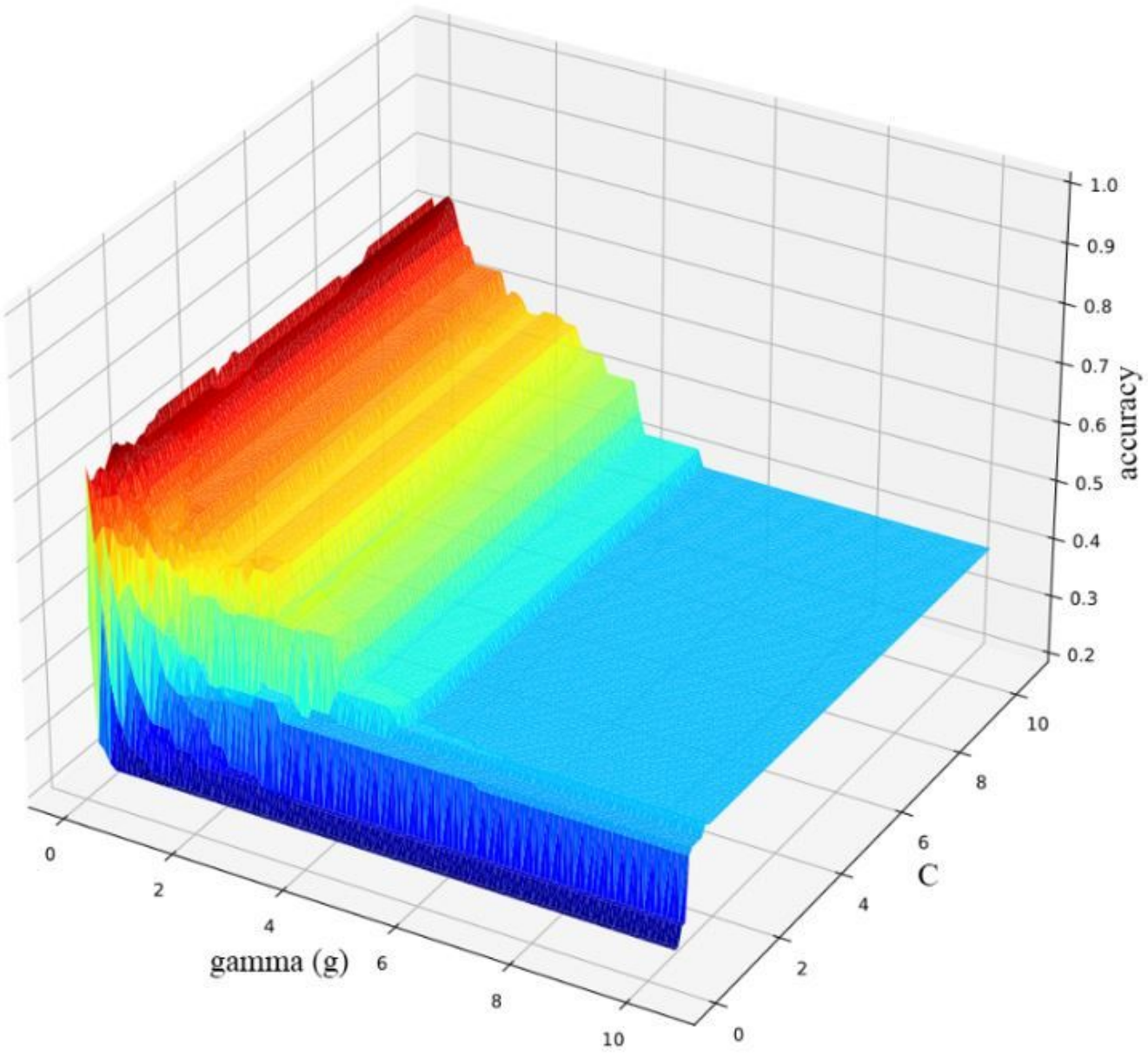

Figure 6

Parameter selection result (difference in seaweed species).

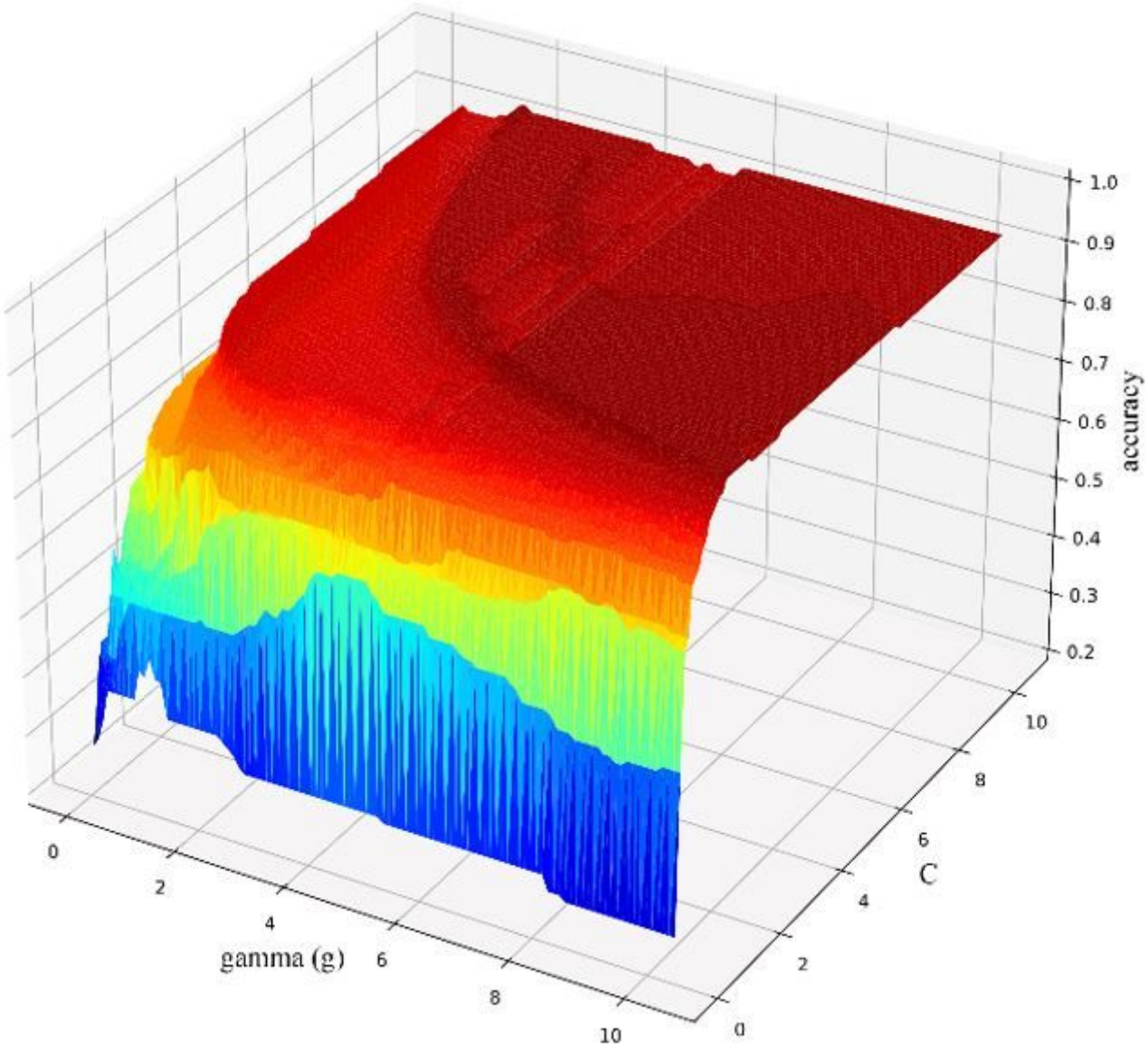

Figure 7

Parameter selection result (different phyla of seaweed).

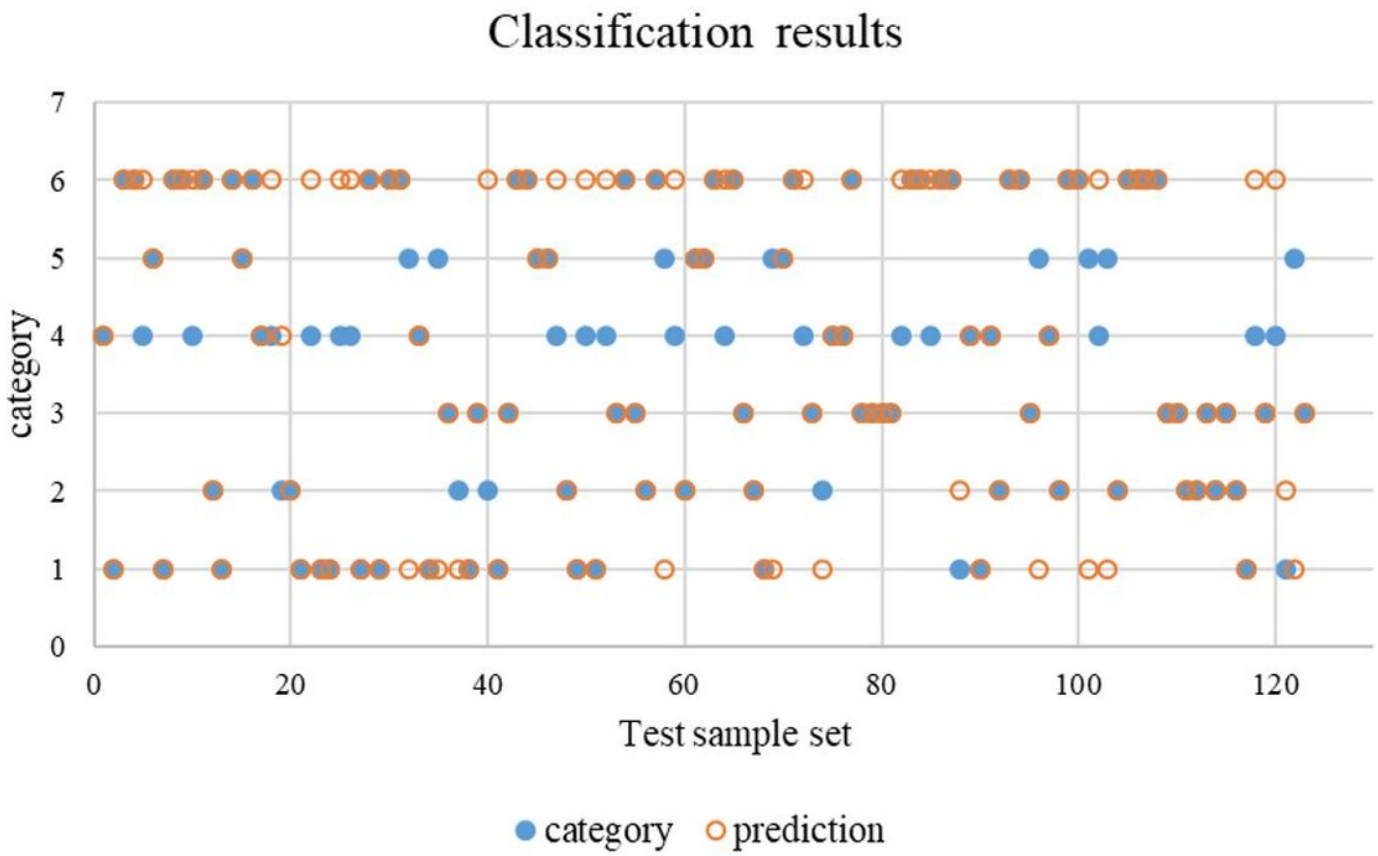

Figure 8

Classification results

Supplementary Files

This is a list of supplementary files associated with this preprint. Click to download.

- Supplementarymaterial.docx